

Transmission sputtering by heavy ions

K. H. Ecker* and K. L. Merkle

Materials Science Division, Argonne National Laboratory, Argonne, Illinois 60439

(Received 19 December 1977)

Transmission sputtering yields of single and polycrystalline gold foils have been measured as a function of thickness in the range 250–5000 Å for bombardments with 560-keV Bi, 400-keV Ag, 200- and 400-keV Ar, and 50-keV He ions. Good agreement is found between the yield curves for polycrystalline and single-crystalline targets oriented in a high-index (random) direction. Calculated distributions of energy deposition in an amorphous target compare well with regard to the position of the maximum in the sputter yield. Absolute yields in the vicinity of the peak are generally in better agreement with yields calculated by Monte Carlo simulation for finite targets than with yields calculated on the basis of transport theory in an infinite solid. Compared with theory, all measured yield curves exhibit considerable enhancement at great depths. Sputter-yield distributions for a beam of 560-keV Bi ions along $\langle 100 \rangle$ are in qualitative agreement with channeling theory. From a comparison with the random sputter-yield distributions, it can be concluded that channeling of such heavy projectiles causes a relatively minor reduction ($\leq 40\%$) in the total amount of energy that goes into nuclear motion.

INTRODUCTION

Great effort has been expended in recent years to investigate the behavior of materials, especially metals under neutron and heavy-ion bombardment, in an attempt to simulate conditions encountered by materials in present and future nuclear reactors. Knowledge of the spatial distribution of energy deposited in the solid under irradiation is of fundamental interest in the understanding of radiation damage and related phenomena such as sputtering.

To date, many of the experimental measurements on *distributions of damage* (i.e., the disorder remaining in the solid after dissipation of the energy) pertain to those visible with the particular detection technique used. Thus, results compared with the *distribution of energy deposition* are prone to errors, due to the effects of defect formation, migration and detectability, which are not always well understood.

At least for the case of metals under heavy-particle irradiation, the sputtering yield, i.e., the number of ejected target atoms per incoming ion, is thought to be directly proportional to the energy deposited at the surface of the solid in the form of target nuclei motion as a result of a collision cascade.¹

For normal incidence of an ion of energy E on a target, the forward or backward sputtering yield S from a surface located at X is given according to Sigmund¹ by

$$S(X, E) = \Lambda F(X, E), \quad (1)$$

where the factor $\Lambda \equiv 3/4\pi^2 NC_0 U_0$ contains parameters describing target properties only. Here N is the density of target atoms, U_0 is the surface

binding energy, and C_0 is a constant that depends on the interaction potential between target atoms. When taking U_0 as the sublimation energy and C_0 from a Born-Mayer-type potential,¹ $\Lambda = 0.187$ (Å/eV) for the Au targets considered in the present experiment.

The ion-target interaction is reflected in the energy-deposition function $F(X, E)$. With $F(X, E)$ calculated on the basis of linear transport theory applied to an infinite target, Eq. (1) has been used successfully¹ to describe a number of back-sputtering yields, that is $S(X=0)$.

It has been shown^{2,3} that, by measuring the sputtering yield in transmission as a function of target thickness, the distribution F of energy deposition can be obtained, particularly the deep penetrating tail of the distribution for which deviations due to the finite target thickness are less severe. The collision cascade cannot fully develop when the target thickness is of the order of or less than the mean projected range of the bombarding particles in an infinite solid. Despite this, even for targets thinner than the projected damage range, fair agreement among experimental³ transmission sputtering yields versus target thickness and theoretical^{1,4} distributions of energy deposition has been found for the case of 6-MeV Au³⁺ and 500-keV Ar⁺ bombardment of Au foils.

It is the objective of the present communication to report suitable experiments that demonstrate the power and limitations of transmission sputtering as a technique to determine the distribution of the energy deposition.

The range of ion species and energies was chosen to elucidate some apparent discrepancies between theory and experiment. For heavy energetic ions (i.e., 500-keV self-ions in Au), some

dechanneling⁵ experiments seem to suggest damage distributions with ranges up to three times those expected from theory. Transmission-electron microscopy (TEM) observations indicate that the peak of the damage is at slightly greater depths than predicted by the random theory⁶ and the mean damage depth is greater than the most probable depth.⁶ In addition, backscattering experiments with molecular ions⁷ indicate that non-linear effects may be significant in such dense cascades.

Sputtering by light ions in the lower keV energy region is of special interest in connection with fusion-reactor technology. Reliable experiments are scarce and large deviations from theory^{4,8} are not uncommon. Thus, some experiments were performed with He⁺ at 50 keV (the lowest feasible energy with our accelerator). The experiments performed with Ar and Ag ions not only probe the deposited energy densities for cascades in between the self-ion and light-ion case but also permit comparison with previous sputtering experiments.

EXPERIMENTAL

The sputtering yield was measured by collecting the sputtered material on carbon foils and then analyzing the deposit by He-ion backscattering (for a review of this technique see Ref. 9). The backscattering method¹⁰ was chosen first for its high sensitivity, which is essential for thin-film transmission sputtering where only a little target material is available and second for the fact that the analysis can be performed in situ, which permits several successive experiments with the same target. At our typical operating conditions for backscattering analysis (10^{-7} A of 200-keV He⁺), a deposit of 2×10^{12} atoms/cm² (i.e., 10^{-3} monolayers) Au on 200- to 800-Å-thick carbon collectors could be determined to an accuracy of better than 20% within 10^3 sec. Thus with the present collection geometry and assuming a cosine emission of sputtered material, only 10^{-2} monolayers of the target have to be removed for one measurement. Irradiation fluences ranged from $\sim 10^{11}$ ions/cm² for 560-keV Bi to $\sim 10^{14}$ ions/cm² for 50-keV He. These fluences are considerably smaller than in most previous sputtering experiments, and systematic errors due to ion implantation, segregation, and surface roughening are kept small. The problems of collection efficiency and resputtering, inherent to this method, were previously shown² to be insignificant for the system Au on carbon.

The experiment was performed at the 300-keV heavy-ion accelerator at Argonne National Labor-

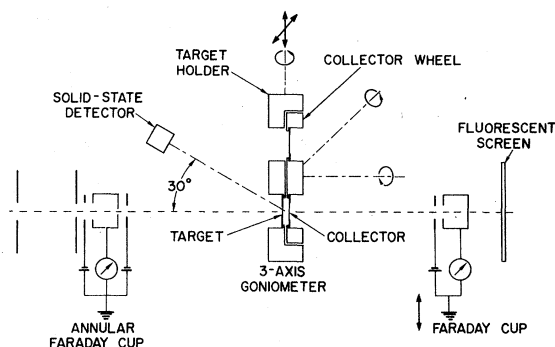


FIG. 1. Schematic showing the experimental arrangement of the transmission-sputtering experiment.

atory. The setup used is shown schematically in Fig. 1. The magnetically analyzed beam was collimated with two pairs of slits and an annular Faraday cup acting as the final aperture. The beam was scanned to assure uniform beam intensity over the annular cup. The increased beam divergence (0.05°) could be tolerated since critical angles for channeling are $>4^\circ$ for all ion-energy combinations in the present experiment. For calibration, an additional Faraday cup could be moved into the beam behind the annular cup. The fluence was measured to an accuracy of better than 3%. Sputtering and backscattering analysis was performed in an ion pumped target chamber operating at 10^{-8} -Torr base pressure, rising to 10^{-7} Torr as a result of predominantly rare gases during beam operation. Au targets and carbon collectors, five each at a time, were mounted on a three-axis goniometer. Two axes were used for orientation of the target with respect to the beam, while, on the third axis, the wheel holding the collectors could be rotated against the targets. During sputtering the distance between target and collector was 1.5 ± 0.1 mm. Through translation of the entire goniometer assembly, any of six positions could be brought into the beam. One position on both the target holder and the collector wheel was left empty to allow backscattering analysis of the collectors and target alignment, respectively. Particles backscattered by 150° were detected by a surface barrier detector with 10-keV energy resolution for 200-keV He ions. The backscattering analysis was calibrated by means of thin film standards from electron-probe analysis¹¹ (EPA) to an absolute accuracy of better than 10%. In order to resolve Au deposits from possible deposits of transmitted Bi or Ag atoms, some collectors were also analyzed by EPA after the sputtering experiment.

Details of the preparation and structure of the single-crystal film have been described previous-

ly,² the only difference being that the targets for the present experiment were grown under improved vacuum conditions. The targets were prepared in an ion pumped vacuum system by vapor deposition on silver-coated rocksalt or glass substrates. The polycrystalline foils had grain sizes $\leq 1 \mu\text{m}$, and no texture could be seen by electron diffraction. After dissolving the Ag in dilute nitric acid and washing in distilled water, the films were picked up directly on aluminum disks with a 1-mm-diam aperture hole. Up to $\sim 1000 \text{ \AA}$, films could be obtained that were stretched flat by surface tension. Thicker films usually had wrinkles, but the films could be stretched¹⁰ by a small dose (10^{12} ion/cm^2) of heavy-ion bombardment. The target thickness up to 2000 \AA was measured by three methods; gravimetry, measurement of the energy loss of 400-keV He ions *in situ* before and during sputtering, and electron-probe analysis after the experiment. Above 2000 \AA only gravimetry was used. The absolute accuracy of the

thickness determination is better than 10% and the relative accuracy better than 5%. To remove adsorbed contaminants from the target surface, sputter cleaning by 200-keV He or 400-keV Ar ions in transmission was employed prior to the sputtering experiment. For the He and Ar experiments, an increase in the yield up to a factor of 2 was observed until about one monolayer of the target was cleaned off, similar to previous observations of Au sputtering by low-energy ions^{2,12}. For the Bi and Ag ions, however, the sputtering yield did not change within experimental error. To avoid additional damage before the experiment, this cleaning procedure was omitted in the case of Bi sputtering from aligned samples. Combined Auger-electron spectroscopy (AES), low-energy electron diffraction (LEED), and molecular-beam scattering has previously shown that an Au surface once "clean" remains in that condition for several hours, even in a moderate vacuum of 10^{-8} Torr, provided the vacuum is free of hydrocarbons.

The single-crystal foils were aligned visually by observation of the star pattern of the transmitted He beam on a fluorescent screen. This procedure proved as accurate as alignment by He backscattering but was much faster and a lower fluence (i.e., $10^{14} \text{ ions/cm}^2$) of He ions was required, thus reducing initial damage. For the single-crystal experiments in random orientation, special care was taken to avoid planes and minor axes. An orientation 15° off the $\langle 100 \rangle$ axis in a zone 22° off the $\{100\}$ zone (see inset in Fig. 5) was maintained to $\pm 0.5^\circ$ for all random experiments.

RESULTS AND DISCUSSION

Typical examples of the amount of transmission sputtered material versus bombarding fluence

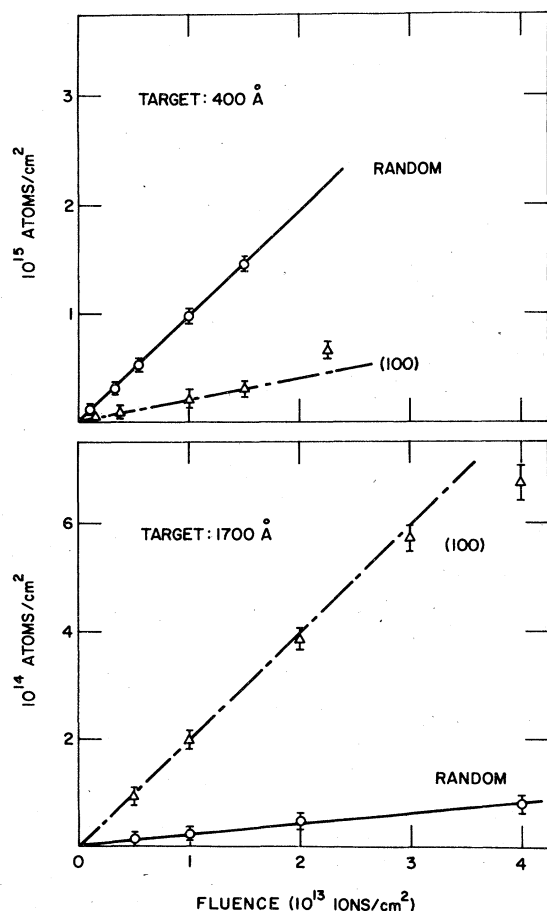


FIG. 2. Transmission-sputtered material as a function of irradiation fluence for 560-keV Bi ions on Au single crystals.

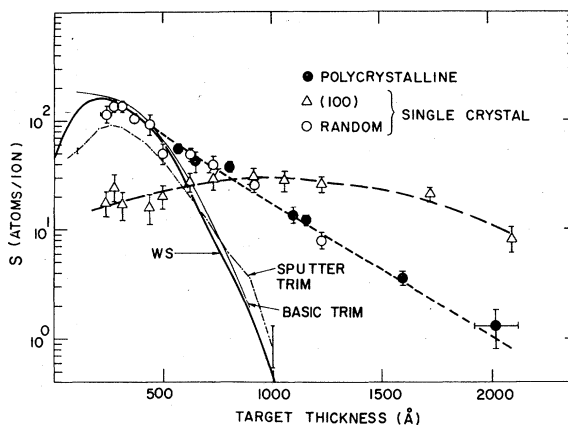


FIG. 3. Transmission-sputtering yield as a function of target thickness for 560-keV Bi on Au.

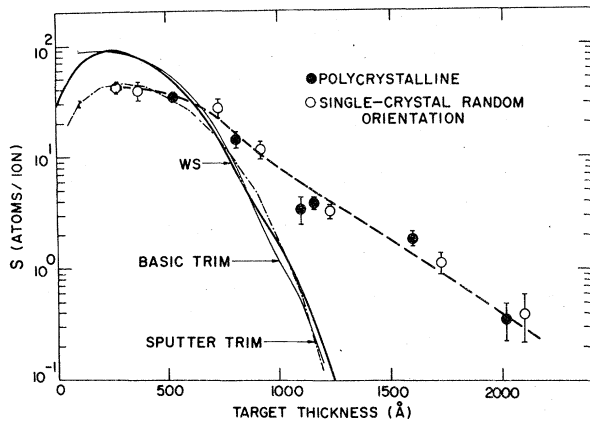


FIG. 4. Transmission-sputtering yield as a function of target thickness for 400-keV Ar on Au.

are shown in Fig. 2 for 560-keV Bi^{3+} irradiation of two (100) Au foils of different thicknesses. Only the counting statistical errors of the backscattering analysis are indicated as error bars. Although linearity within these errors is found for all experiments on single-crystal targets in random orientation and on polycrystals, deviations are observed for (100) oriented targets at fluences above $\sim 10^{13}$ ions/cm². TEM observations^{5,13} have shown a dense network of defect clusters after irradiation with similar fluences of 560-keV Au ions. Thus, deviations of the sputtered amount versus fluence above or below the linear relationships in Fig. 2 for thin or thick targets, respectively, may be interpreted qualitatively as evidence for increased dechanneling at defect clusters. The slope of the initial linear portion of the curves was taken as the experimental sputtering yield.

Transmission sputtering yields as a function of target thickness X are presented in Figs. 3–7. Individual error bars show the statistical errors in

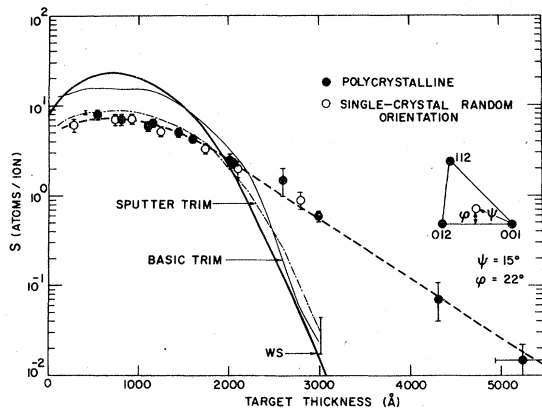


FIG. 5. Transmission-sputtering yield as a function of target thickness for 400-keV Ar on Au.

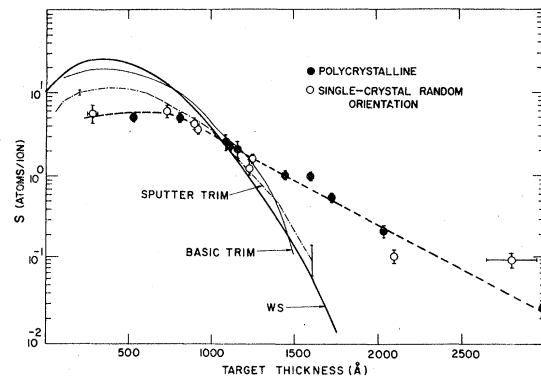


FIG. 6. Transmission-sputtering yield as a function of target thickness for 200-keV Ar on Au.

the trace analysis and the maximum absolute error of the thickness determination at both ends of the distributions. To calculate the amount of sputtered material from the measured deposit on the collector, the angular distribution of the flux of sputtered particles must be known. Due to lack of experimental data for transmission sputtering we have assumed a cosine distribution as expected from theory¹ and from Monte Carlo simulations for a "random" target. To check this assumption the distance between target and collector (1.5 ± 0.1 mm for most experiments) was altered from 0.5 to 5 mm for a few experiments on polycrystalline samples. The sputter yields obtained were consistent with a cosine distribution. The uncertainty in the collection geometry could yield an error of 15% in S . Thus, the absolute accuracy of the sputtering yield is estimated to be 20%, which was also found to be the limit of reproducibility. The broken lines along the experimental points are only intended to guide the eye. Included

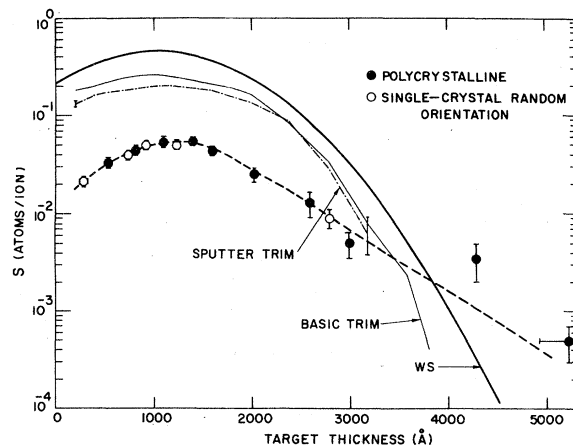


FIG. 7. Transmission-sputtering yield as a function of target thickness for 50-keV He on Au.

in Figs. 3-7 are calculated sputter yields for "random" targets. The thick solid lines represent yields based on Eq. (1) with $F(X)$ as calculated by transport theory in an *infinite* target (WS)^{4,8}. To account for the effects of *finite* target size, Monte Carlo simulations^{14,15} were carried out which follow the particles through the target until they leave through one of the surfaces or until they are stopped inside the target. The first approach (BASIC TRIM) registers the kinetic energies transferred from the incident ion to the first generation of target recoils. From the values of the energy deposit at the surface for targets of different thickness sputter yields are calculated again with Eq. (1) (thin solid lines, Figs. 3-7). The second approach (SPUTTER TRIM) follows the histories of all knock on atoms. In addition to the energy deposit, the number of target particles crossing the surface per incoming ion is calculated (dashed-dotted lines in Figs. 3-7).

The BASIC TRIM code does not take into account the transport by recoils. Thus particularly for the heavy ions Bi and Ag (Figs. 3 and 4) at high energies, that is at low-target thickness before the ions have been slowed down, we note a marked difference in the shape of the curves compared to transport theory and SPUTTER TRIM calculations. However, for lighter ions and at lower energies, the BASIC TRIM calculations give yields close to the SPUTTER TRIM results (see, for example, Fig. 7), thus improving transport theory^{4,8} by allowing for finite target thickness and with an order-of-magnitude shorter computation times compared to SPUTTER TRIM.

The computer program utilized here is particularly fast through energy dependent free flight paths, analytic evaluation of scattering angles, and maintaining only directional information with respect to the surface normal. A Thomas-Fermi-Moliere interaction potential is used and the electronic stopping formulation of Lindhard *et al.*¹⁶ is employed except for knock-ons below 500 eV for which electronic stopping is neglected. Particles which are sputtered have to overcome a planar surface barrier, $E_1 > U_0$ with $U_0 = 4$ eV, the sublimation energy for Au. Further details of the Monte Carlo simulation are described in Refs. 14 and 15.

ION BEAM IN RANDOM ORIENTATION

The following observations were made when the sputtering was performed with the ion beam incident on a single crystal 15° off $\langle 100 \rangle$ (random orientation as described above) or on a polycrystalline specimen.

(i) Within experimental error, no difference in

transmission-sputtering yield was observed between experiments on (100) foils in random orientation and polycrystalline foils.

(ii) All distributions show a tail that falls off roughly exponentially and penetrates far deeper than expected from random cascade theory. This tail is thought to be due to a small number of ions that become channeled. The magnitude of this effect is similar in single and polycrystalline targets. This is to be expected when, as in the present experiments, the grain size in the polycrystalline targets is larger than the foil thickness. It should be noted that, when the experimental and theoretical distributions are compared, the total excess energy in the tail increases as the ion mass increases, but is still <20% even for Bi on Au.

(iii) Within experimental error, the maxima positions of the distributions agree with the calculations for amorphous targets. For the experiments with Bi and Ag, the maxima are not well defined due to lack of experimental points at small target thicknesses. Nevertheless, it is clear that quite long damage ranges, i.e., up to three times the theoretical values, seen by Pronko and co-workers⁵ are not observed in the present experiment. In this connection, it should be noted that the present experiment, in contrast to other methods, for observing displacement energy deposition is not sensitive to damage saturation nor defect migration effects. Particularly when irradiations are carried to high doses and are performed at finite temperatures, both of these effects can result in damage distributions that are substantially different from the as-deposited displacement density distributions.

(iv) The absolute values of the experimental yields near the peak are in much better agreement with the proper Monte Carlo simulations using SPUTTER TRIM¹⁵ than with the yields calculated with the BASIC TRIM code¹⁴ or with transport theory.^{4,8} The differences are mainly due to the loss of primary particles and recoils through the foil surfaces. For 400-keV Ar and 400-keV Ag ions, the agreement is good. Compared to the transmission sputter yield for 500-keV Ar on Au as measured by Bay *et al.* our yield for 400-keV Ar is smaller by a factor 2 to 3, although from the difference in energy a slightly larger yield is expected. This discrepancy could be due to the fact that the irradiation fluence used in the present experiment is lower by at least a factor 10². This would be consistent with the increase of sputter yields with increasing fluence as observed in back-sputtering yields.^{12,17} EerNisse¹⁷ has discussed in detail the dependence of his yields on the fluence. In the present experiment with fluences

about one tenth of his lowest fluences, hopefully true low fluence data are obtained, that is only small changes in surface topography, composition, and binding energy occur. For 560-keV Bi, the experimental yields are roughly 50% higher than the simulated yields. For He, the experimental yields are still approximately four times too low when compared with the calculated yields. It is interesting to note that a steady increase in the ratio of experimental-to-theoretical yields occurs when going from 50-keV He to 200-keV Ar to 400-keV Ar to 400-keV Ag and to 560-keV Bi. Back-sputter yield observations show similar trends in regard to the deviations from sputter theory.^{7,17} The very low He yields are not understood at present. It should be pointed out, however, that the absolute magnitude of our observed He yields at small thickness is consistent with the 45-keV He back-sputter yield measurements by ErNisse.¹⁷ His yield measurements show a strong increase in yield with fluence, but his lowest dose point ($S_{He}=0.046$), which although taken at a fluence considerably above our highest one, nevertheless is only slightly higher than what could be expected for a back-sputter yield on the basis of the data in Fig. 7 when taking into account the influence of finite target thickness. This rather good agreement seems to indicate that our measurements were taken well within the true low fluence regime. For heavy ions, the trend of increasing yields in the series above is consistent with an expected increase in collective emission effects from Ar to Ag and Bi, due to spike phenomena.¹⁸ It has been suggested that spike phenomena may be associated with high-energy-density subcascades.¹⁰ Direct evidence for this has recently been obtained by transmission electron microscopy which has revealed the existence of small craters (~5 nm in diameter) formed in individual energetic displacement cascades in Au.¹³ Such visible craters, while implying an order of magnitude higher sputter yields from some cascades, nevertheless account for only a small fraction of the total sputter yield. Their existence, however, is clear evidence for highly localized spike phenomena which are also expected to take place on the submicroscopic level. The spatial extent of the crater regions is similar in size to the core of a subcascade and therefore occupies only a very small fraction of the total cascade volume. Since spike effects give a greater than linear increase with energy density,⁷ fluctuations in the deposited energy density within individual cascades are important when considering spike effects. Transport theory refers to the average distributions over very many cascades and therefore does not take into account such fluctua-

tions. Qualitatively the observed sputter enhancement in Au can be understood if we apply the concept of subcascade formation¹⁹ and assume that subcascades above a certain energy give rise to spike effects. Also, for very heavy ions quite high-energy-density subcascades are possible when two subcascades overlap. The probability for this is expected to be high in those regions of a cascade where the primary ion or secondary knock-on atoms are at energies between about twice the subcascade energy ($2E_s \sim 100$ keV in Au)¹⁹ and energies near the peak in the nuclear stopping power (~1 MeV for Au). This is indeed the region of incident ion energies in which the most pronounced sputter enhancements have been found in Au self-ion back-sputter experiments.^{10,20} In the transmission-sputter geometry the observed spike enhancements are not expected to be as great as in back-sputter experiments, because even in very thin specimens once the cascade has penetrated to the exit surface, the cascade energy has been shared among very many atoms. Most of these are of low energy and sufficiently disperse not to cause strong collective behavior. If, however, the cascade is energetic enough to have a significant fraction of the cascade energy at the exit surface in the form of secondaries whose energy is in the above mentioned energy range, spike enhancements can be expected to be significant as in the observations of Bay *et al.*³ These authors find strong spike enhancements for 6.8-MeV Au transmission sputtering at quite large depths while the present Bi-sputtering data on Au give enhancements closer to the peak in the deposited energy function. Both observations are readily understood on a qualitative basis by considering the effect of the incident ion energy. Direct evidence for differences in spike enhancements for back and transmission sputtering comes from the observation that the craters observed by TEM are smaller in number and size at the exit surface than at the incident surface for 560-keV Bi on 650-Å-thick Au.

ION BEAM PARALLEL TO (100)

Figure 3 illustrates the marked difference of Bi-ion sputtering for targets in (100) and random orientation. For the thinnest targets investigated, the yield for (100) aligned foils is ~10% of the random yield. Taking the simple relations of Lindhard's²¹ channeling theory, ~9% of the Bi ions enter the crystal too close to atom strings to become channeled. Thus, it would appear that, for the thin targets and energies of several hundred keV, the channeled Bi ions make virtually no contribution to the sputtering. This agrees with model calculations,²² which show that Bi with energies

>10 keV and well channeled in $\langle 100 \rangle$ Au cannot transfer sufficient energy to target atoms to cause ejection. The behavior of S at greater depth can be understood qualitatively as a combination of two effects, the slowing down and, more important, the dechanneling of originally channeled ions. No quantitative comparison with theory is possible, since for heavy ions the theory of channeling at present is poorly developed.

Thomas *et al.*²³ have reported stereo-electron-microscopy measurements of damage distributions (i.e., visible defect clusters) of Au ions up to 120 keV channeled in Au(100). Although the authors point out the possible perturbation of their distributions due to loss of defects to the surfaces of the target, the distribution for their highest bombarding energy (Ref. 23, Fig. 5), is rather similar to the present result, i.e., a broad distribution with an ill-defined maximum almost five times the theoretical damage range for a random target.

Since the nuclear interactions of a channeled particle are reduced when compared with a particle at random incidence it is of interest to know how much of a reduction in the total nuclear energy deposition is experienced by the average particle that starts in a channeling direction. One expects that the channeled sputtering yields are primarily determined by the dechanneled fraction of the beam. If a channeled energy-deposition function $F_{\langle 100 \rangle}(X, E)$ is introduced, one can use Eq. (1) to evaluate the energy deposition for channeled and random incidences. The damage energy or total nuclear energy deposition $\nu(E)$ by a particle of energy E is given by¹

$$\nu(E) = \int_{-\infty}^{+\infty} F(x, E) dx. \quad (2)$$

Assuming the validity of Eq. (1), we find for the ratio between channeled and random damage energy

$$\nu_{\langle 100 \rangle}(E) / \nu_R(E) \approx \int S_{\langle 100 \rangle}(x, E) dx / \int S_R(x, E) dx. \quad (3)$$

Performing the integration over the sputter-yield curves in Fig. 3 gives $\nu_{\langle 100 \rangle} / \nu_R \approx 0.6$ for 560-keV Bi on Au. It is quite remarkable that the channeled beam shows only a 40% reduction in damage energy. This represents a clear demonstration that channeling is not particularly effective in reducing the damage energy for such heavy projectiles. Therefore, for recoil cascades in which secondaries may be scattered into channels, one expects only a slight reduction in the damage production due to this effect. We can obtain a rough estimate of the order of magnitude of this effect by multiplying the fraction of deposited energy in the

exponential tail for random incidence (Fig. 3) by the reduced damage energy fraction for channeled incidence. We conclude from this that channeling effects cause <8% reduction in the damage energy for a recoil cascade.

CONCLUSIONS

(a) Transmission sputtering is well suited to trace the distribution of energy deposition. Particularly the deep penetrating tail could be measured over two to three orders of magnitude, thus complementing other techniques such as channeling and electron microscopy.

(b) For randomly oriented single crystals and polycrystals, projected damage range and straggling are in agreement with random theory, i.e., quite long mean ranges are not observed. The distributions show an exponential tail. This is thought to be due to a few ions that become channeled beyond the extent of the cascade, as expected from the theory for amorphous targets. Since this tail contains <20% of the total energy that goes into target nuclei motion, it is concluded that random cascade theory still gives a good account of the size of the collision cascade in crystalline targets. However, it should be pointed out that the deep penetrating tail can have a significant influence on the damage distribution when the damage density is carried to near saturation levels in high-dose irradiations.

(c) When comparing the absolute sputter yields it should be noted that the present yields are obtained at low irradiation fluences. For the heavy ions Ar, Ag, and Bi, fair agreement is found between experiments and such calculations for which the loss of particles through the surfaces is considered. Significant sputter-yield enhancement due to spike effects seems to be present, at least for Bi.

(d) For the experiment with 50-keV He, a considerable discrepancy (factor of 4 to 5) is found between experimental and calculated yields.

(e) Yields on (100) oriented single crystals are in qualitative agreement with channeling theory.

(f) Channeling effects that may occur in self-ion or recoil cascades are expected to cause only a small reduction in the total nuclear energy deposition. Therefore, defect production is only slightly reduced, even if channeling is significant in recoil cascades.

ACKNOWLEDGMENTS

The authors would like to thank S. M. T. Kazadi, L. R. Singer, and L. J. Thompson for technical assistance. Thanks are also due J. Biersack and L. Haggmark for providing the TRIM code prior to publication. This work was supported by the U.S. Department of Energy.

*Present address: Hahn-Meitner-Institut für Kernforschung GmbH, Berlin, Germany.

¹P. Sigmund, Phys. Rev. 184, 383 (1969).

²K. H. Ecker, Radiat. Eff. 23, 171 (1974).

³H. L. Bay, H. H. Andersen, and W. O. Hofer, Radiat. Eff. 28, 87 (1976); H. L. Bay, H. H. Andersen, W. O. Hofer, and O. Nielsen, Appl. Phys. 11, 289 (1976).

⁴K. B. Winterbon, *Ion Implantation Range and Energy Deposition Distribution* (Plenum, New York, 1976)

⁵I. Nashiyama, P. P. Pronko, and K. L. Merkle, Radiat. Eff. 29, 95 (1975); P. P. Pronko, Nucl. Instrum. Meth. 123, 249 (1976).

⁶K. L. Merkle (unpublished).

⁷H. H. Andersen and H. L. Bay, J. Appl. Phys. 45, 953 (1974); 46, 2416 (1975).

⁸R. Weissman and P. Sigmund, Radiat. Eff. 19, 7 (1973).

⁹W. K. Chu, J. W. Mayer, M. A. Nicolet, T. M. Buck, G. Amsel, and F. Eisen, Thin Solid Films 17, 1 (1973).

¹⁰K. L. Merkle and P. P. Pronko, J. Nucl. Mater. 53, 231 (1974).

¹¹K. H. Ecker, J. Phys. D 6, 2150 (1973).

¹²J. S. Colligon, C. M. Hicks, and A. P. Neokleous, Radiat. Eff. 18, 119 (1973).

¹³K. L. Merkle, *Thirty-Fifth Annual Proceedings of*

EMSA, edited by G. W. Bailey (Claytors, Baton Rouge, La, 1977), p. 36.

¹⁴J. P. Biersack and L. G. Haggmark, Nucl. Instrum. Meth. (to be published).

¹⁵K. H. Ecker and J. P. Biersack, Proceedings of the Seventh International Conference on Atomic Collisions in Solids, Moscow, 1977 (unpublished).

¹⁶J. Lindhard and M. Scharff, Phys. Rev. 124, 128 (1961).

¹⁷E. P. EerNisse, Appl. Phys. Lett. 29, 14 (1976).

¹⁸P. Sigmund, Appl. Phys. 25, 169 (1974); 27, 52 (1975).

¹⁹K. L. Merkle, in *Radiation Damage in Metals*, edited by N. L. Peterson and S. D. Harkness (American Society for Metals, Metals Park, Ohio, 1976), p. 58.

²⁰H. L. Bay, H. H. Andersen, W. O. Hofer, and O. Nielsen, Nucl. Instrum. Meth. 132, 301 (1976).

²¹J. Lindhard, K. Danske Videnskab. Selskab Mat. Fys. Medd. 34, No. 14 (1965).

²²H. H. Andersen and P. Sigmund, Nucl. Instrum. Meth. 38, 238 (1965); K. Danske Videnskab. Selskab Mat. Fys. Medd. 37, No. 14 (1970).

²³L. E. Thomas, T. Schober, and R. W. Balluffi, Radiat. Eff. 1, 269 (1969).